

## EVALUATION OF ENERGY DISSIPATION CAPACITY OF STEEL FRAMES WITH STEEL SHEAR WALLS

F. Dinu<sup>1,4</sup>, C. Neagu<sup>2</sup> and D. Dubina<sup>3,4</sup>

<sup>1</sup> The “Politehnica” University of Timisoara, Romania  
e-mail: florea.dinu@ct.upt.ro

<sup>2</sup> The “Politehnica” University of Timisoara, Romania  
e-mail: calin.neagu@ct.upt.ro

<sup>3</sup> The “Politehnica” University of Timisoara, Romania  
e-mail: dan.dubina@ct.upt.ro

<sup>4</sup> Romanian Academy, Timisoara Branch

**Keywords:** Performance criteria, steel plate shear wall, energy dissipation,  $q$  factor, over-strength.

**Abstract.** *The papers investigate the behavior of steel frames of dissipative steel shear walls. Both numerical and experimental analyses have been conducted in order to characterize in terms of energy dissipation and to evaluate the  $q$ -factor for design of these structures. The tests have been realized for two series of three-bay and two-storey frames, stiffened of Steel Plate Shear Walls. Specimens have been half-scaled and tested under monotonic and cyclic loading. A numerical model has been calibrated via test results for push over and IDA analyses. Parametric studies have been done on different frame typologies in order to obtain the  $q$  factor for such systems.*

## 1 INTRODUCTION

Steel plate shear walls SPSW have been used as lateral force resisting systems since 70's, but the design specifications were rather incomplete at that time. Throughout the last four decades, numerous research programs and also seismic experiences have confirmed their effectiveness. A major role on their development can be attributed to the introduction of design rules in the code provisions, e.g. AISC, 2005 [1] or NBCC, 2006 [2]. The application of SPSW system in Europe is limited, partly due to the lack of design provisions in seismic code EN 1998-1 [3]. Particularly, there are no recommendations for behavior factor and system overstrength factor, respectively. An additional problem refers to the prediction of the strength and stiffness capacity of the SPSW structures. Design practice requires simple models and conventional analysis software that are available and relatively simple to use. One of the models used to represent the behavior of SPSW is the strip model, developed by Thorburn et al., 1983 [4]. Thus, in order to model the steel plate shear walls, the steel plates are replaced by a series of truss members - strips, parallel to tension fields. A minimum of ten strips per panel are required to adequately represent the tension field action developed in the plate.

In order to address the issues presented above with regards to the performances of SPSW systems, an experimental program was developed at the Politehnica University of Timisoara, Steel Structures Laboratory. Previous research of the authors was focused on numerical investigations on SPSW systems (Dinu et al., 2009, [5]) and comparison to conventional braced systems (i.e. centrally braced frames and eccentrically braced frames). In order to evaluate the influence of beam-to-column connections on the response of the structure, two connection typologies were used, i.e. flush end plate bolted connections and extended end plate bolted connections. Structures were tested monotonically and cyclically. Behavior factors were evaluated from the cyclic test. The strip model developed by Thorburn et al. was modified based on the experimental results. In order to extend the behavior factors evaluated experimentally, a numerical study was performed. The paper summarizes the experimental program and presents the results of the numerical study.

## 2 EXPERIMENTAL TEST ON STEEL PLATE SHEAR WALLS

### 2.1 Test specimens

The steel plate shear wall specimens were extracted from a six story frame structure (Figure 1.a). The two actuators used for the tests have 1000 kN and 500 kN capacity and 360mm stroke, respectively. Due to the stroke limitation, the specimens were half-scaled. The infill plates had thickness of 2mm and 3mm, respectively. The frames are 3500 mm height and 4200 mm wide (between member centerlines) (Figure 1.b). The slenderness ratio of shear walls  $L/t_w$  amounted 595 for 2 mm panels and 397 for 3 mm panels, while the aspect ratio  $L/h$  was 0.75. In order to evaluate the contribution of the boundary frames to the strength and stiffness of the structure, two types of beam-to-column connections were used. According to EN1993-1-8 [6] classification, flush end plate connection was semi-rigid and weak partial strength ( $M_{j,Rd}=0.4M_{b,Rd}$ ) (further refereed as semi-rigid) and extended end plate connection was rigid and strong partial strength, with a capacity almost equal to that of the connected beam ( $M_{j,Rd}=0.9M_{b,Rd}$ ) (further refereed as rigid). The infill panels were bolted connected to the boundary members using fish plates. Table 1 shows the thickness of the infill plates, boundary elements, beam-to-column connection types and type of loading. Table 2 shows the material properties of the specimens. As expected, the actual yield strength of the infill plates and boundary elements are much larger than the nominal values.

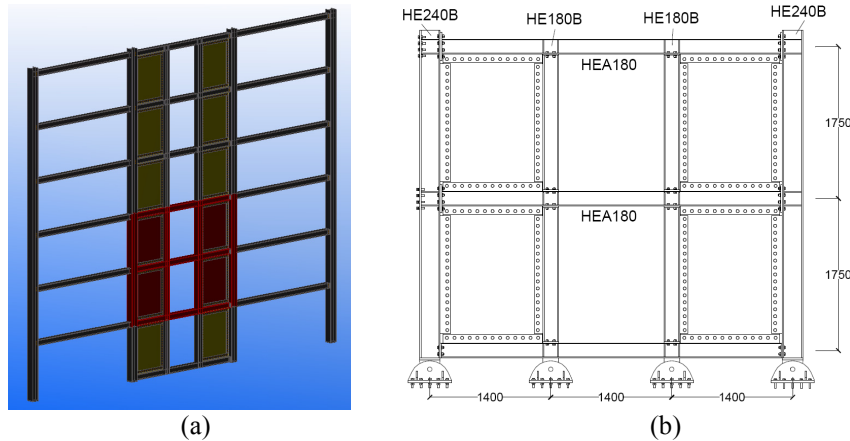


Figure 1: Six story frame structure a) and half-scale test frame b)

Specimen	Infill plate [mm]	Column	Beam	Connection	Loading
R-M-T2	2	HEB240 (HEB180)	HEA180	Rigid	Monotonic
R-C-T2	2			Rigid	Cyclic
SR-C-T2	2			Semi-rigid	Cyclic
SR-C-T3	3			Semi-rigid	Cyclic

Table 1: Design of specimens

Section	Steel grade	Element	$f_y$	$f_u$	$A_u$	Actual steel grade
HEB240	S355	Flange	457	609	40	S460
		Web	458	609	31	
HEB180	S355	Flange	360	515	44	S355
		Web	408	540	40	
HEA180	S355	Flange	419	558	32	S420
		Web	415	542	22.5	
2 mm	S235	Infill plate	305	429	24	S275
3 mm	S235	Infill plate	313	413	25	

Table 2: Material properties

All specimens were tested monotonically and cyclically using ECCS procedure [7] but adapted to particular behavior of steel plate shears walls. The difference is the slope of initial stiffness. Thus, in the original procedure, a monotonic test is done first, in order to evaluate the force-displacement curve that is used to evaluate the equivalent yield displacement. Yield displacement  $D_y$  and corresponding yield force  $F_y$  are obtained by intersecting the initial stiffness  $\alpha_y$  and a tangent at the curve  $F-D$  with a slope of 10% of the initial stiffness. Yield displacement  $D_y$  is then used to calibrate the cyclic loading history. This contains four elastic cycles ( $\pm 0.25D_y$ ,  $\pm 0.5D_y$ ,  $\pm 0.75D_y$  and  $\pm 1.0D_y$ ), followed by groups of 3 cycles of amplitudes multiple of  $2D_y$  ( $3 \times 2D_y$ ,  $3 \times 4D_y$ ,  $3 \times 6D_y$ , ...). Based on experimental results, the evaluation of yield displacement was adjusted to take into account the specific behavior of SPSW. Thus, the slope of initial stiffness was corrected and amounted 20% of the initial stiffness.

## 2.2 Monotonic test

All specimens exhibited stable force-displacement behavior. Figure 2 shows the behavior of the specimen R-M-T2 during the monotonic test. VIC-3D digital image correlation system was used for measurement of shape, displacement and strain. Areas delimited by dashed lines, magnified and represented at the right-hand side of the figures, have the dimensions of 450

mm by 550mm. As the infill plate thickness was small, some out-of-plane deflections occurred due to the fabrication (Figure 2.a), amounting approximately 8.8 mm ( $0.0065\sqrt{Lh}$ ), where  $L$  is the distance between boundary columns centerlines and  $h$  is the story height. Up to inter-story drifts of about 0.5%, specimens were almost elastic. After this drift, some yield lines appeared in the infill plates (Figure 2.b). Out-of plane deflections corresponding to this drift were about  $0.017\sqrt{Lh}$ . Some local cracks were initiated at the corners of the panels at interstory drifts of approximately 2%. The beam-to-column connections presented no damages before plastic deformations took place in panels. Local plastic deformations started to initiate at the beam flange in compression for drifts larger than 2%. For the peak capacity, the interstory drift amounted 6% approximately, while out of plate deflections amounted  $0.02\sqrt{Lh}$  (Figure 2.c). The test was stopped at a top displacement of 240mm as the force started to drop, before the attainment of full shear wall capacity (Figure 3).

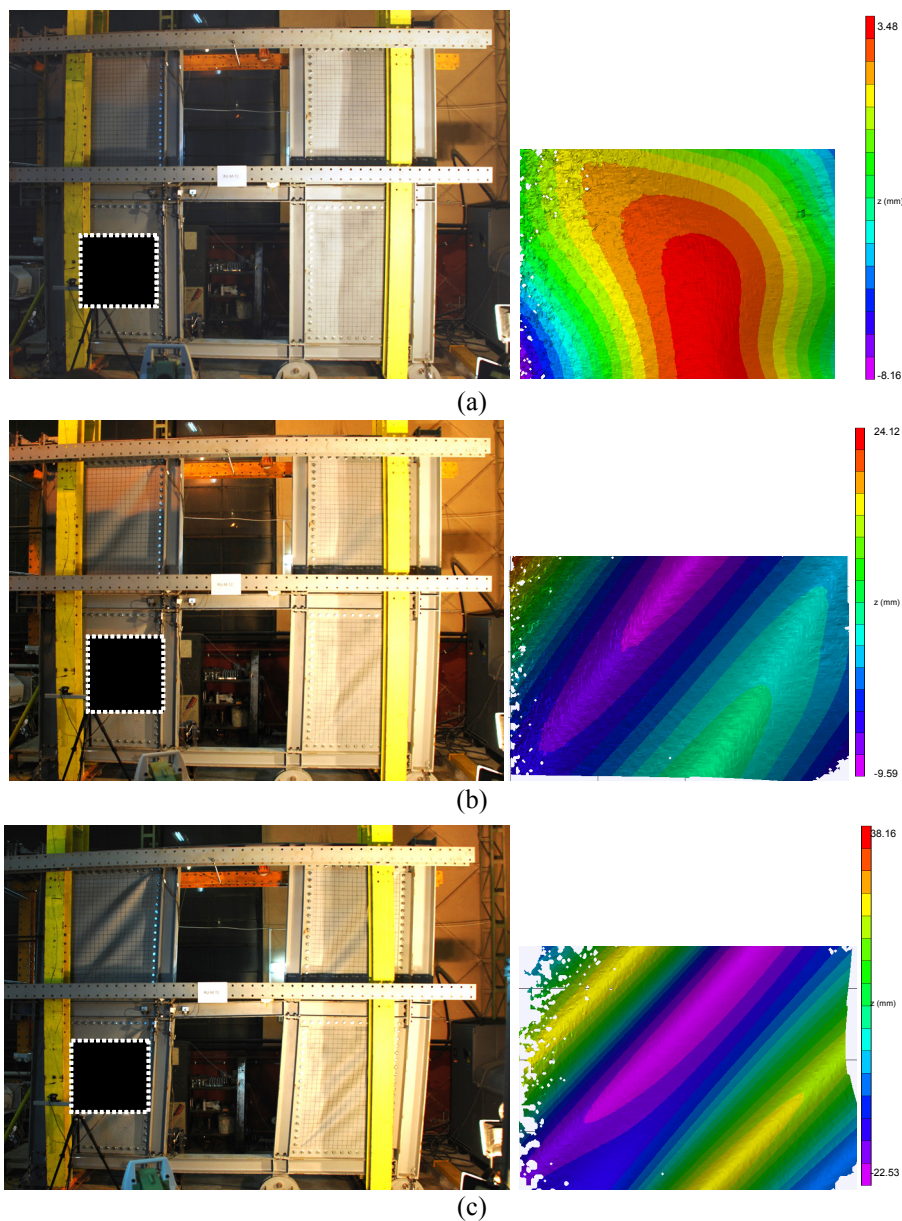


Figure 2: General view and details of the R-M-T2 specimen (VIC measurements with the scale on the right): a) initial state; b) yielding state; c) peak capacity

Results of the monotonic test were compared with the results of a pushover analysis. The strip model used in the pushover analysis was in good agreement with the initial stiffness but underestimated the strength with about 42%. When the plastic hinge was calibrated according to experimental behavior, the accuracy of the model was very much improved (Figure 3). This reduction of the panel area conservatively reduces the design strength and stiffness of the structure.

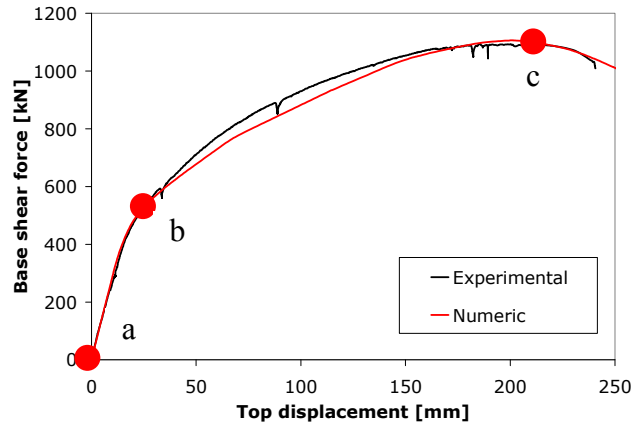


Figure 3: Comparison of experimental results for rigid specimen with 2mm thick panel and numerical results using the strip model

If Figure 2 and Figure 3 are compared, it may be seen the infill plate has out-of-plane deflections in the initial state, see Figure 2.a (it corresponds to point (a) in Figure 3). At yielding, the multiple buckle wavelengths are already visible, see Figure 2.b (it corresponds to point (b) in Figure 3). When the peak capacity is reached, the maximum out-of-plane deflections are doubled compared to yielding state, see Figure 2.c (it corresponds to point (c) in Figure 3).

### 2.3 Cyclic tests

In the cyclic tests, all specimens exhibited stable behavior up to cycles of 4% interstory drift. Panels yielded at approximately 0.005 of the story height. Some local cracks were initiated at the corners of the panels at drifts of approximately 2%. Local plastic deformations were observed at the beam flange in compression for rigid connections. Bolted connections between infill panels and the fish plates shown small slippages but no plastic deformations either in plates or bolts. This enabled a very easy dismantling of the steel panels after the test. Associated with a small residual drift (for rigid structure), this can assure an easy intervention to replace the damaged panels after a moderate earthquake. Some pinching was recorded in the hysteresis loops for large drifts and semi-rigid specimens, only. This can be attributed to the bolted connection between boundary beams and columns and not the slippage of the connection between infill panels and fish plates. This is particularly important at the evaluation of the  $q$  factor, as the pinching need to be taken out at the evaluation of the ultimate displacement.

Figure 4 (left) plots the hysteresis of rigid and semi-rigid specimens. Contribution of rigid connections on the ultimate capacity of the specimens is larger than in the monotonic tests. As the initial stiffness is mainly attributed to the panels, differences between rigid and semi-rigid specimens in terms of stiffness are not as important as differences in terms of strength.

The main parameters associated to the global performance of the SPSW systems are the energy dissipation and global ductility (given by behavior factor  $q$ ). The cyclic tests on three SPSW systems with coupling beams have shown significant ductility and energy dissipation

capacity. The specimens were capable of following large number of inelastic cycles, reaching relatively large drift values (beyond 4%). The area enclosed by a hysteresis curve is a measure of the energy dissipated by the system during a loading cycle. The hysteresis curves of all specimens are fairly wide, indicating good energy absorption of the system. In order to assess quantitatively the performance of the test specimens, the energy dissipation was calculated for each test specimen (Figure 4, right).

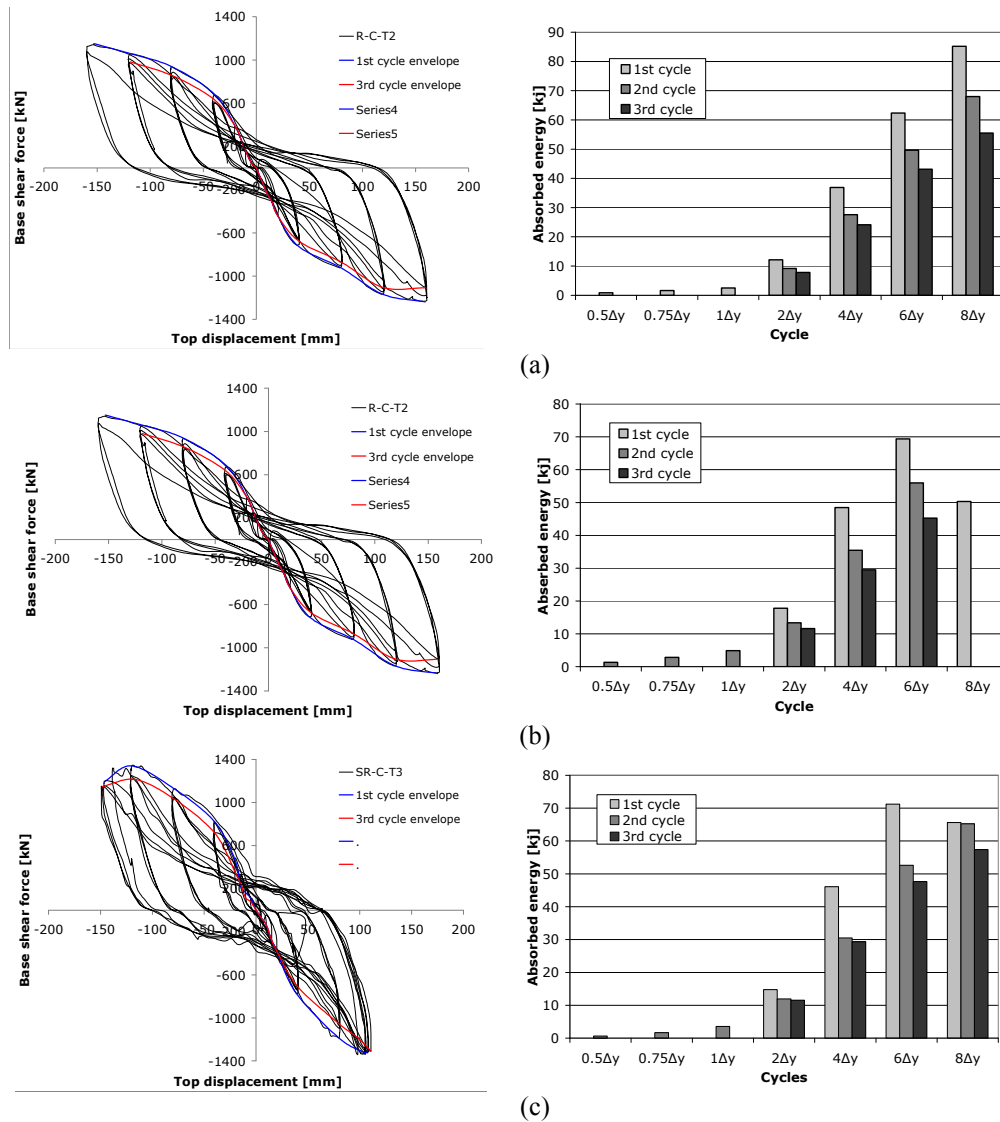


Figure 4: Hysteresis curve and energy dissipation per cycles: a) R-C-T2 specimen; b) SR-C-T2 specimen; c) SR-C-T3 specimen;

An important objective of the experimental program was, also, the evaluation of the behavior factor  $q$ . The  $q$  factor can be expressed as a product of the ductility factor,  $q_{\mu}$ , that accounts for the ductility of the structure and the overstrength factor,  $q_s$ , that accounts for the strength reserve of the structure. The overstrength may vary significantly and is affected by the contribution of gravity loads, material overstrength, structural redundancy, etc. Therefore, in order to calibrate the behavior factor  $q$ , it is more important to focus on the ductility component, which can be taken equal to the displacement ductility factor,  $\mu$ . The ductility reduction factor  $q_{\mu}$  is therefore defined as the ratio of the ultimate displacement  $D_u$  and the yield displacement

$D_y$ . The parameter  $D_u$  corresponds to a reduction of the load carrying capacity of 10% compared to the maximum one. This reduction could be also 20%, but 10% was also imposed by the stroke limitation. The yielding displacement  $D_y$  was evaluated with ECCS methodology and the "stiffness method", where the yield point corresponds to the modification of the elastic stiffness. Based on the observation of the hysteresis curves, the ultimate displacements  $D_u$  for SR-C-T2 and SR-C-T3 were corrected to take into account the pinching during the load reversal. Table 3 presents the  $q_\mu$  factor values for the specimens. Comparing the values obtained with the two methods, it may be seen the specimens have different ductility factors  $q_\mu$ , with values of 4.2 and 5.2. As mentioned before, overstrength factor,  $q_s$ , depends on many factors but for a structural system it can be conservatively evaluated and prescribed in codes. For example, [2] indicates for ductile steel plate shear walls overstrength factor  $R_s$  (equivalent to  $q_s$ ) equal to 1.6. Similar recommendations are given by Berman and Bruneau [8], who recommend an overstrength factor  $R_s=1.5$ . These values show SPSW structures can provide  $q$  factors similar to those corresponding to other dissipative structure, like for example moment resisting frames or eccentrically braced frames.

Structure	$D_y$		$D_u$	$q_u$	
	CEN	stiffness		CEN	stiffness
R-C-T2	38	31	153	4.0	4.9
SR-C-T2	33	26	163	4.9	6.3
SR-C-T3	40	33	147	3.7	4.5
Average value				4.2	5.2

Table 3: q factor values

### 3 EVALUATION OF PERFORMANCE OF STEEL PLATE SHEAR WALL FRAMES

#### 3.1 Design and modeling

In order to assess the performance of steel plate shear wall structures, numerical studies using a nonlinear dynamic procedure were conducted. The geometry of the structure is presented in Figure 5. The interior bays with infill plates consist of either pinned or rigid connections. All stories are 3.5m height. The steel material for the members is S235 ( $f_y=235\text{N/mm}^2$ ), S355 ( $f_y=355\text{N/mm}^2$ ) and S460 ( $f_y=460\text{N/mm}^2$ ). The slenderness ratio  $L/t_w$  and the aspect ratio  $L/h$  of shear walls amount 420 and 0.8, respectively. The design was carried out according to EN1998-1 **Error! Reference source not found.** and P100-1 [9]. For dual frame systems of moment frames and shear walls, EN1998-1 does not provide any recommendations regarding the  $q$  factor. Thus, the results of the experimental program were taken into account,  $q$  factor of 6. A  $4\text{ kN/m}^2$  dead load on the typical floor and  $3.5\text{kN/m}^2$  for the roof were considered, while the live load amounts  $2.0\text{kN/m}^2$ . The buildings are located in a high seismic area (i.e. the Romanian capital, Bucharest), which is characterized by a design peak ground acceleration  $0.24g$  for a returning period of 100 years, and soft soil conditions, with a corner period  $T_C=1.6\text{sec}$ . It is noteworthy the long corner period of the soil, which in this case may affect flexible structures. For serviceability check, the returning period is 30 years, while for collapse prevention it is 475 years. Beams and columns were modeled with plastic hinges located at both ends. The shear walls were modeled with dual strip model, using 10 inclined pin-ended strips, oriented at angle  $\alpha$  in both sides.

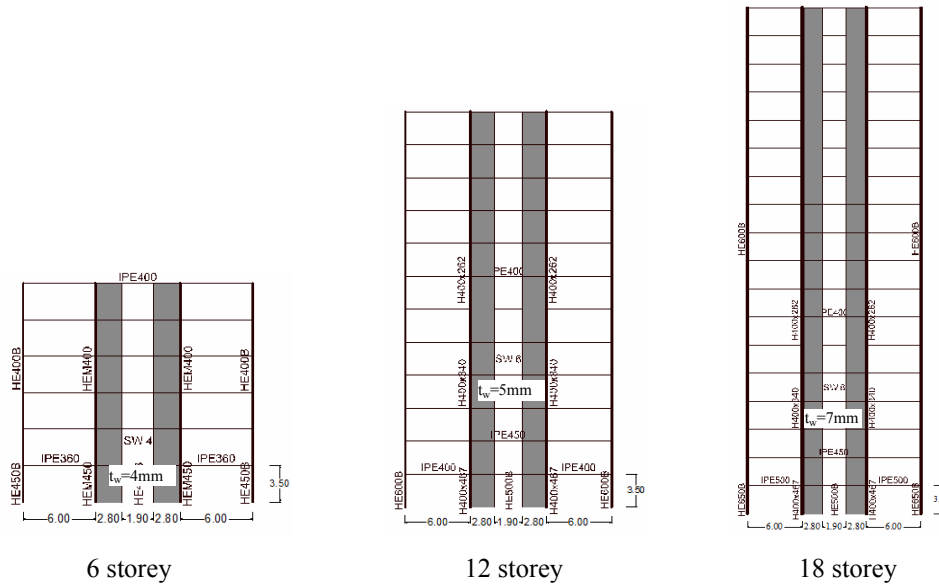


Figure 5: Structural systems investigated in the numerical study

### 3.2 Ground motion records

A set of seven ground motions were used. Spectral characteristics of the ground motions were modified by scaling Fourier amplitudes to match the target elastic spectrum from [9], see Figure 6. This results in a group of semi-artificial records representative to the seismic source affecting the building site and soft soil conditions in Bucharest. The procedure was based on the SIMQKE-1 program (Gasparini & Vanmarcke, 1976) [10].

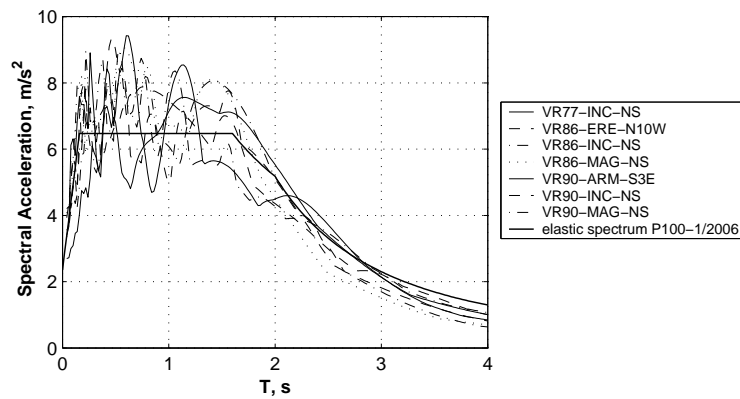


Figure 6: Elastic response spectra of semi artificial records and P100-1/2006 elastic spectrum

### 3.3 Analysis procedure and results

For the evaluation of the behavior factor  $q$ , acceleration time history motion records have been scaled to multiple levels, up to the collapse or the attainment of certain limiting criteria (eg. exhaustion of rotation capacity in elements). Figure 7, Figure 8 and Figure 9 show the maximum interstory drift ratio vs. spectral acceleration  $S_a$  for all structures and records. It can be seen the structure with rigid connections has smaller interstory drifts compared to the structure with pinned connections. The  $q$  factor was defined as the ratio between the acceleration leading to collapse and the acceleration leading to first yielding. Based on the results of the experimental test, first yielding forms in infill plates and corresponds to an interstory drift of 0.5%. The collapse criterion is given by the attainment of dynamic instability or plastic de-



formation capacity of dissipative members, steel panels and beams. For the beams, the plastic rotation capacity was considered 0.035rad. The experimental tests demonstrated that steel panels can sustain an interstory drift of 4%, which is equivalent to 0.035 radian plastic deformation in beams. Table 5 shows the values of  $q_{\mu}$  for rigid and pinned structure. The type of ground motion affects the behavior factor  $q_{\mu}$ . The mean values of the  $q_{\mu}$  factor vary with the height of the structure. 12 and 18 storey structures present almost constant  $q$  factors while the 6 storey structure presents slightly lower values. If these values of the ductility factor  $q_{\mu}$  are combined with the overstrength factors  $q_s$  (see section 2.3) the total  $q$  factor is obtained. It may be seen the design of SPSW structures may use similar behavior factors  $q$  as other dissipative structures, i.e. moment resisting frames.

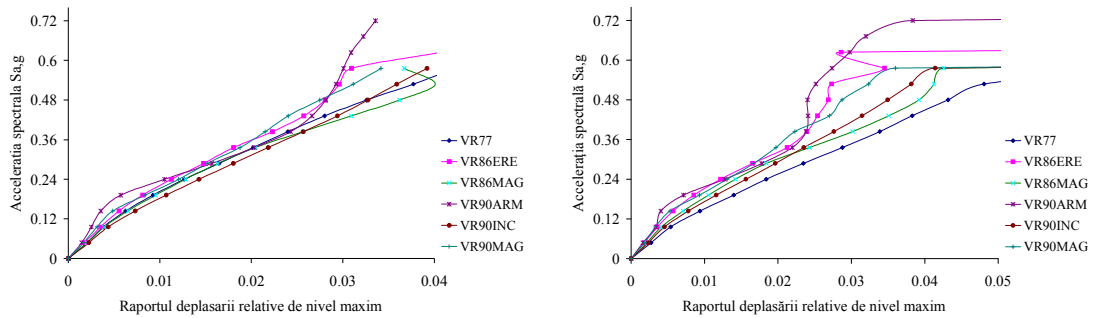


Figure 7: IDA curves: maximum interstory drift ratio vs. spectral acceleration  $S_a(g)$  for all records 6 storey structures: a) Rigid; b) Pinned

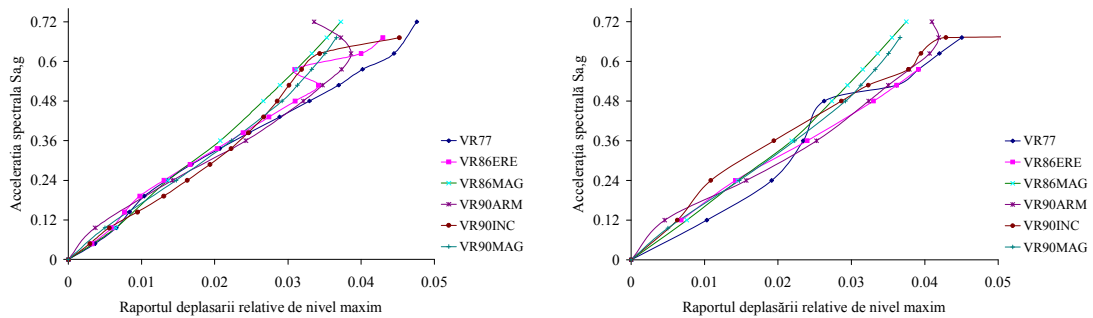


Figure 8: IDA curves: maximum interstory drift ratio vs. spectral acceleration  $S_a(g)$  for all records 12 storey structures: a) Rigid; b) Pinned

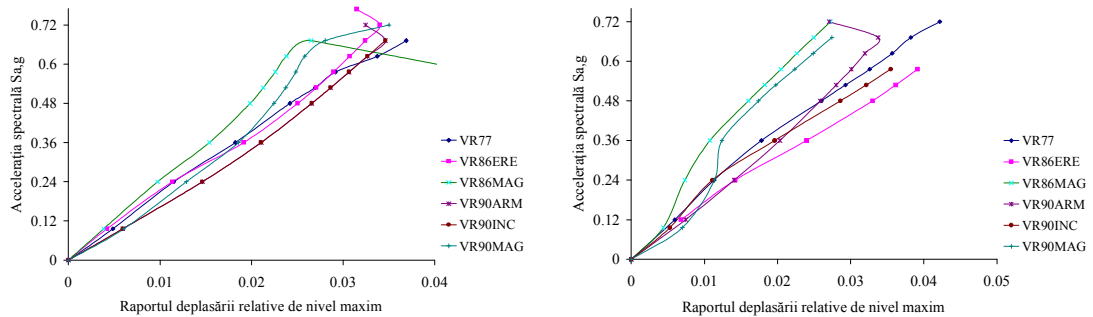


Figure 9: IDA curves: maximum interstory drift ratio vs. spectral acceleration  $S_a(g)$  for all records for 18 storey structures: a) Rigid; b) Pinned

Earth-quake	no. of Storey	Acceler-ation		q	no. of Storey	Acceleration		q	no. of Storey	Acceleration		q	
		a <sub>gy</sub>	a <sub>gu</sub>			a <sub>gy</sub>	a <sub>gu</sub>			a <sub>gy</sub>	a <sub>gu</sub>		
VR77INC	6	0.10	0.58	6.0	12	0.10	0.53	5.5	18	0.10	0.48	5.0	
VR86ERE		0.12	0.62	5.2		0.10	0.58	6.0		0.10	0.77	8.0	
VR86MAG		0.10	0.58	6.0		0.10	0.72	7.5		0.13	0.67	5.1	
VR90ARM		0.12	0.72	6.0		0.10	0.62	6.5		0.10	0.72	7.5	
VR90INC		0.10	0.58	6.0		0.10	0.53	5.5		0.10	0.53	5.5	
VR90MAG		0.12	0.62	5.2		0.10	0.62	6.5		0.10	0.67	7.0	
AVERAGE				5.7					6.3				

Table 4: q factors for structures with rigid connections

Earth-quake	no. of Storey	Acceler-ation		q	no. of Storey	Acceleration		q	no. of Storey	Acceleration		q	
		a <sub>gy</sub>	a <sub>gu</sub>			a <sub>gy</sub>	a <sub>gu</sub>			a <sub>gy</sub>	a <sub>gu</sub>		
VR77INC	6	0.10	0.58	6.0	12	0.10	0.53	5.5	18	0.10	0.48	5.0	
VR86ERE		0.12	0.62	5.2		0.10	0.62	6.5		0.10	0.77	8.0	
VR86MAG		0.10	0.53	5.5		0.10	0.72	7.5		0.12	0.67	5.6	
VR90ARM		0.12	0.77	6.4		0.10	0.72	7.5		0.10	0.72	7.5	
VR90INC		0.10	0.58	6.0		0.10	0.58	6.0		0.10	0.53	5.5	
VR90MAG		0.12	0.67	5.6		0.10	0.62	6.5		0.10	0.67	7.0	
AVERAGE				5.8					6.5				

Table 5: q factors for structures with pinned connections

#### 4 CONCLUSIONS

Experimental and numerical investigations were conducted on dual steel plate shear wall structures. A total of 4 specimens were designed and fabricated, which included specimens of semi-rigid and rigid connections. Specimens were tested monotonically and cyclically. Rigid connections increased the “yield resistance” and the ultimate capacity of the structures. The initial stiffness was also improved when rigid beam-to-column connections were used. Behavior factor  $q$  (considering the contribution of the ductility, only) was evaluated, based on two methods. The  $q$  factor values indicate that SPSW structures exhibit a dissipative behavior, similar to other dissipative structures, like for example moment resisting frames. For extending the results on the behavior factor  $q$  for SPSW structures, a numerical study on different structures was performed. Behavior factor  $q$  varies with the height of the structures and type of ground motion. The mean values of  $q$  factors obtained via numerical analysis are very closed to those resulted from experimental tests.

#### REFERENCES

- [1] AISC 341-05, *Seismic provisions for structural steel buildings*, American Institute for Steel Construction, 2005.
- [2] NBCC, *National Building Code of Canada*, Institute for Research in Construction, National Research Council of Canada, Ottawa, 2005.
- [3] EN 1998-1, *Design provisions for earthquake resistance of structures - 1-1: General rules - Seismic actions and general requirements for structures*, CEN, EN1998-1-1, October 1994.

- [4] L. J. Thorburn, G. L. Kulak and C. J. Montgomery, Analysis of steel plate shear walls. *Structural Engineering Rep. No. 107*, Dept. of Civil Engineering, Univ. of Alberta, Edmonton, Alberta, Canada, 2003.
- [5] F. Dinu, D. Dubina, C. Neagu, A comparative analysis of performances of high strength steel dual frames of buckling restrained braces vs. dissipative shear walls, *Proc. of International Conference STESSA 2009: Behavior of Steel Structures in Seismic Areas, Philadelphia*, 16-20 Aug 2009, CRC Press, Ed. F.M. Mazzolani, J.M. Ricles, R. Sause, ISBN: 978-0-415-56326-0, 2009.
- [6] EN1993-1-8, *Design of Steel Structures. Part 1-8: Design of joints*, CEN, Brussels, 2003.
- [7] ECCS 1985, Recommended Testing Procedures for Assessing the Behavior of Structural Elements under Cyclic Loads. *European Convention for Constructional Steelwork. Technical Committee 1, TWG 1.3 – Seismic Design, No.45*, 1985.
- [8] J. Berman and M Bruneau, Plastic Analysis and Design of Steel Plate Shear Walls. *Journal of Structural Engineering, ASCE, Vol. 129, No. 11*, 2003.
- [9] P100-1, Partea I: Prevederi de proiectare pentru clădiri. *Cod de proiectare seismică P100*, Romania, 2006.
- [10] D.A. Gasparini and E.H. Vanmarcke, Simulated Earthquake Motions Compatible with Prescribed Response Spectra. *Research Report R76-4*. Massachusetts Institute of Technology, Department of Civil Engineering, Cambridge, Massachusetts, 1976.